

# Vibrations and diverging length scales near the unjamming transition

Leonardo E. Silbert\*

*James Franck Institute, University of Chicago, Chicago, IL 60637 and  
Department of Chemistry and Biochemistry, UCLA, Los Angeles, CA 90095*

Andrea J. Liu

*Department of Physics and Astronomy, University of Pennsylvania, Philadelphia, PA 19104*

Sidney R. Nagel

*James Franck Institute, The University of Chicago, Chicago, IL 60637*

(Dated: September 19, 2018)

We numerically study the vibrations of jammed packings of particles interacting with finite-range, repulsive potentials at zero temperature. As the packing fraction  $\phi$  is lowered towards the onset of unjamming at  $\phi_c$ , the density of vibrational states approaches a non-zero value in the limit of zero frequency. For  $\phi > \phi_c$ , there is a crossover frequency,  $\omega^*$  below which the density of states drops towards zero. This crossover frequency obeys power-law scaling with  $\phi - \phi_c$ . Characteristic length scales, determined from the dominant wavevector contributing to the eigenmode at  $\omega^*$ , diverge as power-laws at the unjamming transition.

PACS numbers: 61.43.-j 63.50.+x 64.70.Pf

The jamming/unjamming transition for zero-temperature sphere packings has a mixed first-order/second-order character [1, 2]. This transition occurs for particles with finite-range and purely repulsive interactions. As a system unjams with decreasing packing fraction, the number of interacting neighbors per particle drops discontinuously to zero. Despite this characteristic signature of first-order behavior, power-law scaling is also observed for other quantities [1]. This raises the question of whether there is a diverging length scale associated with the loss of rigidity. Simulations suggest that a diverging length scale exists on the low-density side of the transition [2, 3], but there has been no demonstration of similar behavior in the jammed phase. Because the jamming transition may control the glass transition at higher densities and temperatures [2], an observation of a diverging correlation length should shed light on the nature of the glass transition and properties of glasses in general. Here we show that a diverging length can be extracted from the vibrational properties of the jammed phase.

In most crystalline or amorphous solids, vibrations at low frequency,  $\omega$ , are expected to be long-wavelength, acoustic plane waves. From this assumption one obtains the asymptotic low-frequency Debye density of vibrational states:  $\mathcal{D}(\omega) \propto \omega^{D-1}$  where  $D$  is the dimension of space. A feature of glassy systems is that there is an excess in the density of low-frequency vibrations [4]. There has been an extensive body of simulation work on phonon spectra in quenched glasses dating back to the 1970's [5]. In particular, studies of the Lennard-Jones glass found an increasing number of low-frequency modes as the system was diluted in an *ad-hoc* fashion [6]. Perhaps the most dramatic demonstration of this excess

density of low-frequency modes appears in a system at zero temperature with a well-defined jamming transition at packing fraction  $\phi_c$  [2]. For systems with attractions, the jamming transition is usually inaccessible because of the vapor-liquid phase transition [7]. Therefore, a system with soft, purely-repulsive, finite-range interactions has the advantage of allowing a systematic study of the properties near its well-defined jamming transition.

In the simulations reported here we have studied monodisperse spheres of diameter  $\sigma$  interacting through a finite-range, purely repulsive, harmonic potential:

$$V(r) = \begin{cases} V_0(1 - r/\sigma)^2 & r < \sigma \\ 0 & r \geq \sigma. \end{cases}$$

Here  $r$  is the center-to-center separation between two particles. The units of length and time are  $\sigma$  and  $(m\sigma^2/V_0)^{1/2}$ , respectively, for particles of mass  $m$ . Our three dimensional (3D) systems consist of  $N = 1024$ , 4096, and 10000 spheres in cubic simulation cells with periodic boundary conditions. We employ conjugate-gradient energy minimization in order to obtain  $T = 0$  configurations. We have also studied bidisperse, harmonic discs in  $2D$ , as well as Hertzian contact potentials in  $3D$ . Our conclusions are the same for all three systems.

In Fig. 1(a) we show a log-log plot of the density of states,  $\mathcal{D}(\omega)$  as a function of  $\omega$  covering eight decades in  $(\phi - \phi_c)$  for one system size. For the smallest value of  $(\phi - \phi_c)$  studied, the low-frequency behavior approaches a flat spectrum with an  $\omega = 0$  intercept of  $\mathcal{D}_0 \equiv \mathcal{D}(\omega \rightarrow 0)$ . Thus, close to the jamming transition there is no longer any vestige of Debye behavior. As the system is compressed above threshold, the curves depart from this plateau behavior at a frequency  $\omega^*$ , which increases with

$(\phi - \phi_c)$ . Below  $\omega^*$ ,  $\mathcal{D}(\omega) \rightarrow 0$  as  $\omega \rightarrow 0$ . Experiments on vitreous silica [8] and simulations of models of glasses with three-body interactions [9] have observed a similar trend with decreasing pressure. Figure 1(b) is the full spectrum divided by  $\omega^2$  for all system sizes, at several values of  $(\phi - \phi_c)$ . The peak position in  $\mathcal{D}(\omega)/\omega^2$  shifts to lower frequencies and the peak height increases as  $\phi_c$  is approached, analogous to the way some glasses behave as the glass transition temperature is approached [10]. Thus, our zero-temperature system captures features often associated with the Boson peak in real glasses [11].

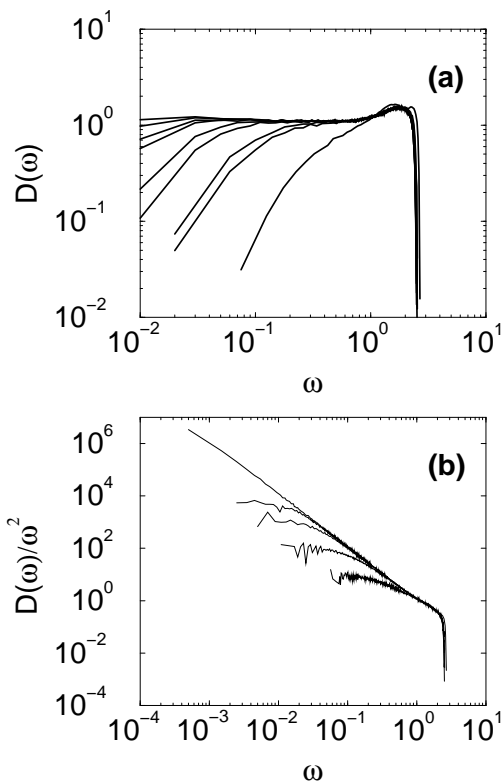


FIG. 1: (a) Density of vibrational states  $\mathcal{D}(\omega)$ , for  $N = 1024$  monodisperse spheres in  $3D$ , interacting via harmonic repulsions. The curves from right to left are for,  $\phi - \phi_c = 1 \times 10^{-1}$ ,  $1 \times 10^{-2}$ ,  $5 \times 10^{-3}$ ,  $1 \times 10^{-3}$ ,  $5 \times 10^{-4}$ ,  $1 \times 10^{-4}$ ,  $5 \times 10^{-5}$ ,  $1 \times 10^{-6}$ ,  $1 \times 10^{-8}$ . (b)  $\mathcal{D}(\omega)/\omega^2$  at  $\phi - \phi_c = 1 \times 10^{-6}$ ,  $1 \times 10^{-4}$ ,  $1 \times 10^{-3}$ ,  $1 \times 10^{-2}$ , and  $1 \times 10^{-1}$ , using data from  $N = 1024, 4096$ , and  $10000$ .

Figure 2 shows the crossover frequency,  $\omega^*$ , versus  $(\phi - \phi_c)$ . We determine  $\omega^*$  by finding where  $\mathcal{D}(\omega)$  for a given  $(\phi - \phi_c)$  departs from  $\mathcal{D}(\omega)$  for the next smallest value of  $(\phi - \phi_c)$ . Over more than 4 decades in  $(\phi - \phi_c)$ ,  $\omega^*$  vanishes as a power law:

$$\omega^* \propto (\phi - \phi_c)^\Omega \quad (1)$$

with  $\Omega = 0.48 \pm 0.03$ . The scaling is robust, independent of the precise manner in which we determine  $\omega^*$ . It is the same (with different prefactors) when  $\omega^*$  is defined as the

value of  $\omega$  at which  $\mathcal{D}(\omega)$  reaches  $D_0$ ,  $0.9D_0$  or  $0.5D_0$ , as well as the frequency where  $\mathcal{D}(\omega)/\omega^2$  in Fig. 1(b) levels off with decreasing  $\omega$ .

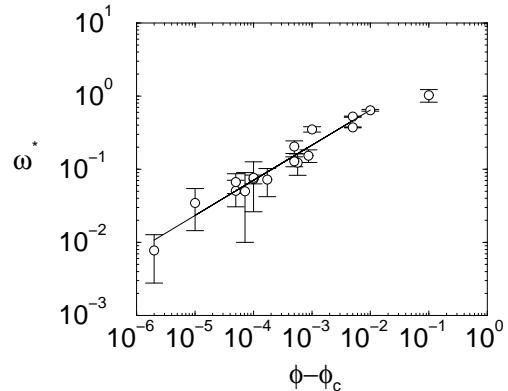


FIG. 2: The crossover frequency  $\omega^*$ . The line is a fit to Eq. 1 with  $\Omega = 0.48$ .

Given  $\omega^*$ , we can define a corresponding length scale,  $\xi_T$ , that diverges as  $\phi$  approaches  $\phi_c^+$ . In order to extract  $\xi_T$  we examine the spatial variation of the eigenmode corresponding to the frequency  $\omega^*$ . We take the Fourier transform of the appropriate component of the polarization vector,  $\mathbf{P}_i(\omega^*)$  of each particle  $i$ , which, for transverse waves is,

$$f_T(k, \omega^*) = \left\langle \left| \sum_i \hat{\mathbf{k}} \wedge \mathbf{P}_i(\omega^*) \exp(i\mathbf{k} \cdot \mathbf{r}_i) \right|^2 \right\rangle,$$

where  $\langle \rangle$  denotes an average over configurations and over all wave-vectors with the same magnitude  $k$ . (The longitudinal component,  $f_L(k, \omega)$ , not shown [12], is the dynamical structure factor accessible from inelastic neutron scattering.) Figure 3(a) shows these functions at the values of  $\omega^*$  determined for different compressions,  $(\phi - \phi_c)$ . The transverse components exhibit well-defined peaks at  $k^*$  at small wavevectors (there is a system size cut-off at  $k_{min} = 2\pi/L$ , where  $L$  is the size of the simulation box). Thus,  $\xi_T \equiv 2\pi/k^*$  is the dominant transverse length scale for that mode. Figure 3(b) shows  $\xi_T$  as a function of  $(\phi - \phi_c)$ . The solid line corresponds to a power-law fit:

$$\xi_T \propto (\phi - \phi_c)^{-\nu_T} \quad , \quad (2)$$

with  $\nu_T = 0.24 \pm 0.03$ . The exponents  $\nu_T$  and  $\Omega$  (Eq. 1) can be related to each other via a simple scaling argument using  $k^* = \omega^*/c_T(\phi)$ , where  $c_T(\phi)$  is the velocity of transverse sound. The shear modulus  $G_\infty$  vanishes with an exponent of  $\gamma = 0.48 \pm 0.05$  [2], implying that  $c_T(\phi)$  vanishes with an exponent of 0.24. Given  $\Omega = 0.48$ , we would therefore expect  $\nu_T = \Omega - \gamma/2 \approx 0.24$ , in agreement with the results of Fig. 3(b).

A similar argument can be constructed for a longitudinal length  $\xi_L$  based on the peak of  $f_L(k, \omega^*)$ . Although

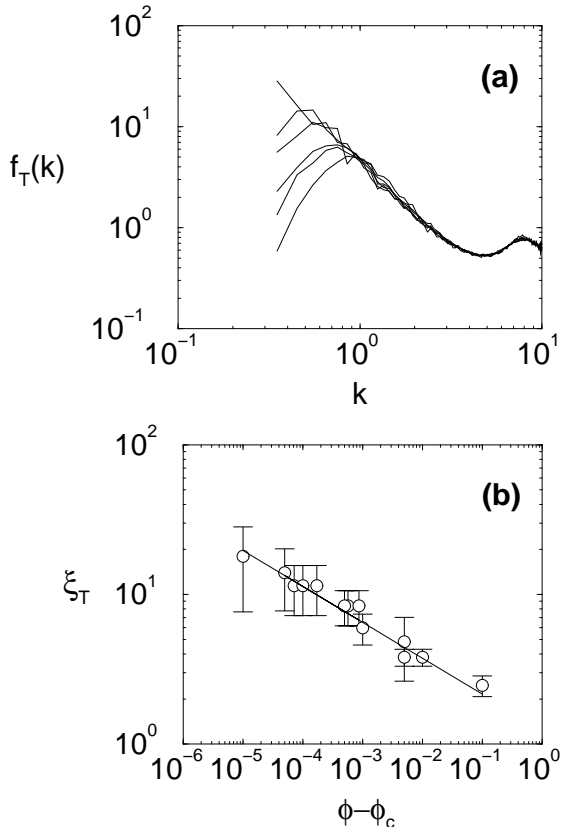


FIG. 3: (a) Transverse spectral functions  $f_T(k, \omega^*)$  for  $\phi - \phi_c = 1 \times 10^{-5}, 5 \times 10^{-5}, 1 \times 10^{-4}, 5 \times 10^{-4}, 1 \times 10^{-3}, 5 \times 10^{-3}$ , with decreasing amplitude respectively. (b) The correlation length  $\xi_T \equiv 2\pi/k^*$  obtained from the wave-vector  $k^*$  for the position of the peak in  $f_T$  at frequency  $\omega^*$ .

it is difficult to extract the peak value from  $f_L(k, \omega^*)$  because the peaks occur at very low values of  $k$ , the analogous scaling relation based on the longitudinal sound speed (and hence the bulk modulus, which is independent of  $\phi - \phi_c$  [2]) predicts

$$\nu_L \approx 0.48. \quad (3)$$

We have also simulated a system with Hertzian potentials:  $V_0(1 - r/\sigma)^{5/2}$ , for  $r < \sigma$ , and zero otherwise. In this case, we find that  $\omega^*$  vanishes with an exponent  $\Omega \approx 0.78 \pm 0.03$ , which is different from that obtained for the harmonic case. However, by calculating the peak of  $f_T(k, \omega^*)$  we obtain a length scale  $\xi_T$  that diverges with  $\nu_T \approx 0.23$ , just as in the harmonic case. This is again consistent with the scaling argument based on the speed of sound, since the shear modulus vanishes with an exponent  $\gamma \approx 0.95$  for the Hertzian case [2]. Thus, even though the scaling of  $\omega^*$  is different for the Hertzian and harmonic potentials, we have the same scaling for  $\xi_T$ .

The strong departure from the low-frequency Debye density of states suggests that the eigenmodes are poorly characterized by simple plane waves [13]. We illustrate

this point in Fig. 4 where we show the lowest frequency modes for 2D harmonic systems at the two extreme values of  $(\phi - \phi_c) = 1 \times 10^{-1}$  and  $1 \times 10^{-8}$ . We show 2D results here for ease of visualization. These correspond to modes below and above  $\omega^*$ , respectively, for those packing fractions. In the compressed system at  $\omega < \omega^*$  the eigenmode retains identifiable correlated plane-wave-like character, consistent with the more Debye-like behavior of  $\mathcal{D}(\omega)$  as  $\omega \rightarrow 0$ . In contrast, when  $\omega > \omega^*$  as in the system closest to  $\phi_c$ , all plane-wave character is lost. This picture suggests that  $\xi_T$  represents the length scale above which one can average over disorder: wavevectors of magnitude  $k > 2\pi/\xi_T$  do not have long enough wavelengths for effective averaging to take place. This is related to the criterion that characterizes the elastic-granular crossover in a Lennard-Jones glass [14].

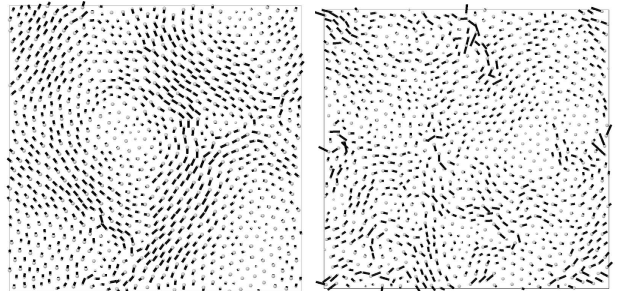


FIG. 4: Lowest frequency eigenmodes for  $N = 1024$  bidisperse discs in 2D, at two extreme values of  $\phi - \phi_c$ :  $1 \times 10^{-1}$  (left), and  $1 \times 10^{-8}$  (right). The dots represent the centers of the particle and the black lines their polarization vectors.

Our results for  $\omega^*$  and  $\xi_T$  motivated two recent theoretical papers that treat different aspects of the zero-temperature jamming transition. The first paper, by Wyart *et al.* [15], shows that the constant density of states is a direct consequence of the system being at what is called an isostatic point, where the number of constraints precisely equals the number of degrees of freedom [1, 2, 16]. This theory predicts  $\Omega = 1/2$  and  $\Omega = 3/4$  for the harmonic and Hertzian potentials, respectively, in excellent agreement with our simulations. It also predicts a new length scale,  $\ell \propto (\phi - \phi_c)^{-1/2}$ . This is not the same scaling as we have found for  $\xi_T$ , but it is consistent with the scaling of  $\xi_L$  predicted by the speed of sound argument (Eq. 3). The length scale defined in Ref. 15 results from a competition between bulk mechanical stability and boundary-induced mode softening, and has not yet been explored by simulation.

A second theory by Schwarz *et al.* [17] makes an analogy between jamming at  $\phi_c$  and the onset of  $k$ -core percolation. The  $k$ -fold coordination required for each site corresponds to the  $D + 1$ -fold coordination required for a particle to be locally stable in  $D$  dimensions. For the Bethe lattice, Schwarz *et al.* [17] find exponents for the number of overlapping neighbors per particle and the sin-

gular part of the shear modulus that are in good agreement with our simulations [1]. Moreover, they find a correlation length exponent of  $\nu = 1/4$ , in agreement with Eq. 2. Interestingly, the Bethe lattice calculations [17] also suggest the presence of another length scale with an exponent of  $\nu^\# = 1/2$ , in possible agreement with predictions of Wyart *et al.* [15] and our argument for  $\xi_L$ .

O'Hern *et al.* [1, 2] found another correlation-length exponent by measuring the shift in the peak of the distribution of jamming thresholds as the system size increases [1, 2]. This exponent was measured to be  $\tilde{\nu} \approx 0.7$  in both 2 and 3 dimensions. Finally, yet another diverging length scale has been measured in simulations by Drocco *et al.* [3] as the jamming threshold is approached from below. They measured the distance over which a slowly-moving particle disturbs the surrounding packing and found  $\nu_- = 0.6 - 0.7$ , in good agreement with the finite-size scaling results of O'Hern *et al.* [1, 2].

There are at least three length scales that are important in describing the jamming/unjamming transition: (i) The interparticle overlap distance, which goes to zero at  $\phi_c$  with a power-law exponent of approximately 1.0 [2]. (ii) the length scale determined from finite-size scaling [1, 2] as well as the length [3] calculated as the transition is approached from low densities. These diverge with an exponent of roughly 0.7. (iii) the diverging length scale presented here on the high-density side of the transition, determined from transverse vibrations; this diverges with an exponent of 0.24. Theories [15, 17] and a scaling argument based on our data (Eq. 3) suggest a fourth length scale with exponent 0.5. It is still not clear how all these different length scales are tied together. That different exponents are observed on different sides of the transition suggests that the jammed phase may always be separated from the unjammed one by a singularity.

Disordered or glassy systems characteristically show an excess in the number of low-energy excitations. In particular, there is a Boson peak that can increase in magnitude and shift to lower frequency as the glass transition is approached [8, 10]. However, nowhere are these two effects more clearly demonstrated than at the onset of unjamming. There  $\mathcal{D}(\omega)$  approaches a constant as  $\omega \rightarrow 0$  instead of dropping to zero, implying, as shown in Fig. 1(b), that the Boson peak diverges and the peak position,  $\omega^*$ , shifts all the way to zero frequency as the rigidity disappears. This is in accord with random-network theories [18] and numerical studies imposing disordered force constants on a lattice [19]. The behavior we observe is clearly associated with the critical nature of the transition and thus provides a natural way of describing these effects in terms of a diverging length scale. Our studies also indicate that the enhancement of the low-frequency modes is purely a geometrical phenomenon.

In conclusion, we have studied the properties of the jamming/unjamming transition at zero temperature. Despite the discontinuity in the number of interacting

neighbors, we find that the loss of rigidity is characterized by a diverging length scale. Moreover, we note that the jump in the number of interacting neighbors is universal, and given by the isostatic condition. This indicates that unjamming may be described as a second-order transition with a universal jump in the order parameter.

We thank Lincoln Chayes, Gary Grest, Corey O'Hern, Jennifer Schwarz, Thomas Witten, and Matthieu Wyart for insightful discussions. We gratefully acknowledge the support of NSF-DMR-0087349 (AJL), NSF-DMR-0352777 (SRN), DE-FG02-03ER46087 (AJL,LES), and DE-FG02-03ER46088 (SRN,LES).

---

\* Electronic address: lsilbert@uchicago.edu

- [1] C. S. O'Hern, S. A. Langer, A. J. Liu, and S. R. Nagel, *Phys. Rev. Lett.* **88**, 075507 (2002).
- [2] C. S. O'Hern, L. E. Silbert, A. J. Liu, and S. R. Nagel, *Phys. Rev. E* **68**, 011306 (2003).
- [3] J. A. Drocco, M. B. Hastings, C. J. O. Reichhardt, and C. Reichhardt, arXiv:cond-mat/0310291.
- [4] W. A. Phillips, ed., *Amorphous solids, Low temperature properties* (Springer, Berlin, 1981).
- [5] A. Rahman, M. J. Mandell, and J. P. McTague, *J. Chem. Phys.* **64**, 1564 (1976).
- [6] S. R. Nagel, G. S. Grest, S. Feng, and L. M. Schwartz, *Phys. Rev. B* **34**, 8667 (1986).
- [7] S. Sastry, P. G. Debenedetti, and F. H. Stillinger, *Phys. Rev. E* **56**, 5533 (1997).
- [8] Y. Inamura, M. Arai, T. Otomo, N. Kitamura, and U. Buchenau, *Physica B* **284-288**, 1157 (2000).
- [9] O. Pilla, L. Angenlani, A. Fontana, J. R. Goncalves, and G. Ruocco, *J. Phys.:Condens. Matter* **15**, S995 (2003); K. Trachenko, M. T. Dove, V. Brazhkin, and F. S. Elkin, *Phys. Rev. Lett.* **93**, 135502 (2004).
- [10] A. P. Sokolov, U. Buchenau, W. Steffen, B. Frick, and A. Wischnewski, *Phys. Rev. B* **52**, R9815 (1995).
- [11] S. R. Elliott, *Physics of Amorphous Materials* (Longmans, New York, 1990), 2nd ed.
- [12] L. E. Silbert, A. J. Liu, and S. R. Nagel, unpublished.
- [13] L. E. Silbert, C. S. O'Hern, A. J. Liu, and S. R. Nagel, in *Unifying concepts in granular media and glasses*, edited by A. Coniglio, A. Fierro, H. J. Herrmann, and M. Nicodemi (Elsevier, Amsterdam, 2004).
- [14] J. P. Wittmer, A. Tanguy, J.-L. Barrat, and L. Lewis, *Europhys. Lett.* **57**, 423 (2002); A. Tanguy, J. P. Wittmer, F. Leonforte, and J.-L. Barrat, *Phys. Rev. B* **66**, 174205 (2002).
- [15] M. Wyart, S. R. Nagel, and T. A. Witten, arXiv:cond-mat/0409687.
- [16] C. F. Moukarzel, *Phys. Rev. Lett.* **81**, 1634 (1998); J.-N. Roux, *Phys. Rev. E* **61**, 6802 (2000).
- [17] J. Schwarz, A. J. Liu, and L. Q. Chayes, arXiv:cond-mat/0410595.
- [18] T. S. Grigera, V. Martin-Mayor, G. Parisi, and P. Verrocchio, *J. Phys.:Condens. Matter* **14**, 2167 (2002).
- [19] W. Schirmacher, G. Diezemann, and C. Ganter, *Phys. Rev. Lett.* **81**, 136 (1998); S. N. Taraskin, Y. L. Loh, G. Natarajan, and S. R. Elliott, *Phys. Rev. Lett.* **86**, 1255 (2001).